International Global Navigation Satellite Systems Association
IGNSS Conference 2018

Colombo Theatres, Kensington Campus, UNSW Australia
7 – 9 February 2018

An Indoor-Outdoor Cooperative Localization Framework for UAVs

Salil Goel
Joint PhD Student (MIPA Scholar)
Department of Infrastructure Engineering
The University of Melbourne, Australia
and
Department of Civil Engineering
Indian Institute of Technology Kanpur, India
Email: goel.salilg@gmail.com

Jelena Gabela
PhD Student
Department of Computing and Information Systems
The University of Melbourne, Australia
Email: jgabela@student.unimelb.edu.au

Allison Kealy
Professor
Department of Spatial Sciences
RMIT University, Australia
Email: allison.kealy@rmit.edu.au

Guenther Retscher
Associate Professor
Department of Geodesy and Geoinformation
TU Wien, Vienna, Austria
Email: guenther.retscher@tuwien.ac.at

ABSTRACT

Positioning and navigation in urban environments has been challenging due to partial unavailability of GNSS (Global Navigation Satellite Systems) measurements. The increasing availability of Wi-Fi (Wireless Fidelity) and UWB (Ultra-Wide Band) measurements in indoor as well as outdoor urban environments provides additional measurements that could be used for localization. It has been demonstrated that sharing of information among multiple platforms can help to overcome the challenges of precise localization in GNSS challenging environments. This information sharing strategy referred to as 'Cooperative Localization (CL)' has been shown to provide superior localization solution in GNSS available environments. CL refers to simultaneous positioning of all dynamic platforms in a connected network where each node shares information about its own state and some relative information about other nodes. A CL framework that combines information exchange among multiple platforms and measurements from GNSS, UWB and Wi-Fi can potentially solve some of the positioning and navigation challenges in urban and indoor environments.

This paper develops an indoor-outdoor CL framework and a prototype for Unmanned Aerial Vehicles (UAVs) using low cost sensors such as MEMS (Micro Electro-Mechanical Systems) Inertial, GNSS, UWB and Wi-Fi. This system uses information exchange among multiple static nodes and dynamic nodes in both indoor and outdoor environments to achieve a seamless indoor-outdoor localization solution. Preliminary results of our ongoing efforts to develop this system indicate that proposed system can achieve accuracy of the order of ~2-5 m in challenging GNSS environments. The framework developed in this research is aimed at achieving ubiquitous positioning and may prove to be helpful in applications such as exploration, search and rescue, disaster management, situational awareness, assisted guidance and navigation, etc.

KEYWORDS: Cooperative Localization, Unmanned Aerial Vehicles, Wi-Fi, UWB, Extended Kalman Filter

1. INTRODUCTION

Global Navigation Satellite Systems (GNSS) are now being used by almost all the segments of the society in multiple applications including mapping, positioning and navigation, tracking, search and rescue, robotics, autonomous cars and virtually every possible application that requires either positioning or navigating in outdoor environments. GNSS works efficiently and infallibly in clear outdoor environments where a direct line of sight between the satellite and the receiver can be established. Under obstructed environments such as urban canyons, forests, tunnels or indoor environments, positioning and navigation still remains a challenging problem. An integration of inertial sensors such as Inertial Measurement Unit (IMU) with GNSS has helped resolve the problem of partial GNSS availability for shorter periods of time. In the cases of extended GNSS unavailability, the positioning solution diverges due to accumulation of biases in the inertial measurements. Thus, an integrated GNSS/IMU solution cannot be used in indoor environments. However, the rise of alternative measurements derived from signals such as UWB (Ultra-Wide Band) and other signals such as Wi-Fi (Wireless Fidelity) that were not actually intended for positioning has enabled users to derive localization solutions in urban and indoor environments (Retscher and Tatschl 2016). The existing literature demonstrates that extensive research has been performed in Wi-Fi positioning methods (Retscher and Tatschl 2016, Schauer *et al*. 2013, Xiao *et al*. 2011) as well as integration of various complimentary technologies such UWB, GNSS, and IMU. A new paradigm called 'Cooperative localization' (CL) makes use of information from multiple sensors installed on multiple platforms for estimating the joint positioning solution for all platforms (Bailey *et al*. 2011). It has been demonstrated that CL may result in improvement in localization accuracy as compared to a platform relying only its on-board sensors (Goel *et al*. 2017a). A majority of the developed solutions are aimed at either indoor or outdoor environments where the dynamic platforms are operating only in one kind of environment. From a practical perspective, it is very much possible that a platform (such as Unmanned Aerial Vehicle (UAV)) moves from indoor to outdoor environment or some of the platforms in a cooperative network are operating in indoor environments while others are outdoors. A change in the environment of a platform affects the type as well as the quality of measurements that become available to it. For example, GNSS measurements are available only to the platforms (UAVs) in outdoor environments while Wi-Fi measurements may be available in both indoor and outdoor environments. The quality of UWB measurements in indoor environments may be poorer (compared to outdoor environment) due to NLOS (Non Line of Sight) conditions as well as

multipath effects. All such factors can have a significant impact on the localization accuracy of a specific UAV (platform) in a cooperative network as well as the overall network. Some of the previous works have demonstrated the advantage of cooperative localization in partially GNSS denied environments (Goel 2017, Goel *et al*. 2017a, Caceres *et al*. 2010), benefits of including measurements from Wi-Fi and UWB in a cooperative network (Goel *et al*. 2016c, Caceres *et al*. 2010) and the improvement in the positioning accuracy due to inclusion of infrastructure based nodes (Goel *et al*. 2016b). The existing cooperative localization systems include sensors such as GNSS (Caceres *et al*. 2010, Goel 2017), UWB, Wi-Fi, Camera (Indelman *et al*. 2011), Laser range finder (Madhavan *et al*. 2002), etc. on platforms such as ground robots (Bailey *et al*. 2011, Caceres *et al*. 2010, Madhavan *et al*. 2002) and UAVs (Goel 2017, Goel *et al*. 2017b). A majority of the existing cooperative localization systems ignore IMU observations (Karam *et a*l. 2006), assume planar 2D environments (Roumeliotis and Bekey 2002, Caceres *et al*. 2010) and slow moving platforms (Madhavan *et al*. 2002). Various estimation methods and algorithms such as Extended Kalman Filter (EKF) (Goel 2017, Goel *et al*. 2017a), Belief Propagation (Caceres *et al*. 2010, Savic *et al*. 2010), Covariance Intersection (Carrillo *et al*. 2013), etc. have been proposed for cooperative localization. Although Belief propagation and covariance intersection have been demonstrated to work well in simulation studies, their implementation in a practical problem has been rather limited (Goel 2017). Therefore, this paper uses a centralized EKF framework to include Wi-Fi and UWB measurements in a cooperative network from static and dynamic nodes to develop and analyse an indoor-outdoor cooperative localization system for UAVs. Some of the applications of this framework (and system) include search and exploration, situational awareness, assisted navigation, etc. The next section presents the details of the sensor setup for cooperative localization in a multi-platform and multi-sensor system. Section 3 explains the complete mathematical framework for fusion of observations from multiple sensors (such as GNSS, IMU, Wi-Fi, UWB etc.) as well as multiple (static or dynamic) platforms in a cooperative environment. The simulation setup and network is presented in section 4. The results of the simulations performed using this setup are presented and analysed in section 5. Finally, the conclusions of this paper and some ideas for future work are presented in section 6.

2. SENSOR SETUP FOR THE PROPOSED FRAMEWORK

The sensor setup for indoor-outdoor cooperative localization framework includes five UAV platforms all of which are installed with low-cost GNSS, IMU, UWB, Camera and Wi-Fi sensors. Further, this framework incorporates static infrastructure nodes including Wi-Fi Access Points (AP) and static UWB nodes. A generalized sensor setup for the proposed framework is shown in Figure 1. A total of five UAV platforms are seen in this Figure, of which one UAV is operating in indoor environments. The lines connecting any two UAVs or any UAV with any infrastructure node (Wi-Fi AP or UWB) denotes a communication link and the ability of the UAV to receive and transmit relevant information. The UAV with ID 5 is able to communicate with the other four UAVs that are outdoors and can receive GNSS measurements. Additionally, the UAV inside the room can receive measurements from Wi-Fi AP and UWB nodes inside the room/building. The objective of this framework is then to jointly estimate the states of all UAVs in the network, after taking into account all observations. This is especially challenging and important for the UAV operating inside the building since it cannot receive any GNSS measurements. In this setup, it is assumed that the location of all infrastructure nodes including Wi-Fi AP and UWB nodes is known in advance. The details of some of the sensors proposed to be used in this research on-board on the UAVs are listed in Table 1. A similar cooperative network that is developed using the sensors

mentioned in this table and is demonstrated in outdoor environments is presented in Goel (2017). It is to be noted that the inclusion of measurements from static infrastructure nodes in a cooperative network results in a significant improvement in the positioning solution of the dynamic UAVs (Goel *et al*. 2016b, Goel *et al*. 2016c, Goel *et al*. 2017b). This is the primary motivation behind using static UWB nodes in the proposed setup. Further, such infrastructure nodes are readily available in urban environments and thus, can be utilized effectively. In summary, any UAV in the above mentioned cooperative network can receive following observations,

1. Inertial observations (angular rate and accelerations) from on-board sensors
2. GNSS measurements from satellites (if visible)
3. Distance measurements from static UWBs
4. RSS measurements from Wi-Fi AP
5. Relative range measurements from neighbouring UAVs.
6. State and covariance information of the neighbouring UAVs.

The above mentioned measurements in this setup are fused using an EKF to jointly estimate the state (and covariance) of all UAVs. The next section presents the mathematical framework based on EKF for cooperative localization.

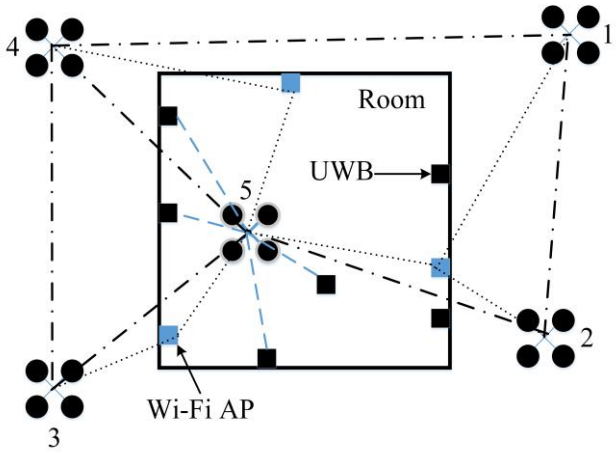

Figure 1: Plan view of a general setup of a multi-platform cooperative localization system.

Table 1: Details of sensors installed on each UAV in the cooperative network (after Goel 2017).

On-board Sensors	Dimensions	Weight	Approx. Cost
Raspberry Pi 3	85.6mm x 56.5 mm	45 grams	50 USD
uBlox GPS	38mm x 38mm x 8.5 mm	16.8 grams	140 USD
Pixhawk	81.5mm x 50mm x 15.5mm	38 grams	200 USD
P410 UWB	76mm x 80mm x 16mm	58 grams	100 USD
GoPro Camera	60mm x 42mm x 30mm	74 grams	300 USD

3. FRAMEWORK FOR INDOOR-OUTDOOR COOPERATIVE LOCALIZATION

This section presents the mathematical setup, framework and models for developing a ubiquitous cooperative localization system for both indoor and outdoor environments. As explained in the previous section, each UAV is equipped with inertial sensors. The measurements from these sensors are used for state prediction. Once either GNSS measurements, or relative measurements (Wi-Fi or UWB) from either static or dynamic nodes becomes available, the predicted state is updated. The next section explains the state prediction step based on inertial observations and a mobility model, followed by fusion of relative and absolute measurements in the cooperative network.

3.1 UAV State Vector and Mobility Model

The mobility model provides a mathematical model for the motion of the UAVs in a cooperative network. The mobility model in this case encompasses the time evolution of the state vector of all UAVs in a swarm. This time evolution of the UAV state includes observations from the inertial sensors (accelerometers and gyroscopes) on-board each platform. The state vector X_k of the complete cooperative swarm at an instant k includes the state of all the cooperating UAVs and is given by the following equation.

$$X_k = \left[\left(x_k^1\right)^T \quad \left(x_k^2\right)^T \quad . \quad . \quad \left(x_k^{i-1}\right)^T \quad \left(x_k^i\right)^T \quad . \quad . \quad \left(x_k^N\right)^T \right]^T \tag{1}$$

In this equation, the state vector of the i^{th} UAV at an instant k is denoted by x_k^i. The superscript T denotes the transpose of a vector. This state vector is composed of UAV position (r_k^i), velocity (v_k^i), attitude (α_k^i) and biases from accelerometer ($b_{a,k}^i$) and gyroscope ($b_{g,k}^i$). This state vector can be mathematically expressed by the following equation.

$$x_k^i = \left[\left(r_k^i\right)^T \quad \left(v_k^i\right)^T \quad \left(\alpha_k^i\right)^T \quad \left(b_{a,k}^i\right)^T \quad \left(b_{g,k}^i\right)^T \right] \tag{2}$$

The mobility model of any UAV in a cooperative swarm is governed by the kinematic equations of motion given in equations (3) to (5). In these equations, the rate of change of a vector x with respect to time is denoted by $\dot{x}$. In the following equations, the accelerometer and gyroscope observations are denoted by f_b and ω_{ib}, respectively. The earth rotation vector and its corresponding skew symmetric matrix is denoted by ω_{ie} and Ω_{ie}^e, respectively and the constant gravity vector is denoted by g_e. These equations are expressed in ECEF (Earth Centered Earth Fixed) frame which is denoted by the subscript e, while the inertial sensor observations are recorded in the local body frame that is denoted by b. The rotation matrix R_b^e denotes a rotation from local body frame to the ECEF frame, comprises the attitude of the UAV and is given by equation (6). Based on the below kinematic equations, the authors in Goel *et al*. (2017a) and Goel *et al*. (2016a) demonstrated that the state transition matrix F_k^i and matrix G_k^i for each UAV can be computed as given in equations (7) and (8), respectively. Further, the joint state transition matrix F_k and joint G_k matrix is given as a diagonal matrix of individual F_k^i and G_k^i matrices and is given in Goel *et al*. (2016a) and Goel *et al*. (2017a).

$$\dot{r}_e = v_e \tag{3}$$

$$\dot{v}_e = R_b^e f_b - 2\Omega_{ie}^e v_e + g_e \tag{4}$$

$$\dot{\alpha}_e = \begin{bmatrix} \dot{\phi} \\ \dot{\theta} \\ \dot{\psi} \end{bmatrix} = \begin{bmatrix} 1 & \sin\phi\tan\theta & \cos\phi\tan\theta \\ 0 & \cos\phi & -\sin\phi \\ 0 & \sin\phi\sec\theta & \cos\phi\sec\theta \end{bmatrix} \left(\omega_{ib} - \omega_{ie}\right) \tag{5}$$

$$R_b^e = \begin{bmatrix} \cos\theta\cos\psi & \sin\phi\sin\theta\cos\psi - \cos\phi\sin\psi & \sin\phi\sin\psi + \cos\phi\sin\theta\cos\psi \\ \cos\theta\sin\psi & \cos\phi\cos\psi + \sin\phi\sin\theta\sin\psi & \cos\phi\sin\theta\sin\psi - \sin\phi\cos\psi \\ -\sin\theta & \sin\phi\cos\theta & \cos\phi\cos\theta \end{bmatrix} \tag{6}$$

$$F_k^i = \begin{bmatrix} I_{3x3} & I_{3x3}\Delta t & 0_{3x3} & 0_{3x3} & 0_{3x3} \\ 0_{3x3} & \left(I_{3x3} - 2\Omega_{ie}^e \Delta t\right) & -\frac{\partial\left(R_b^e b_a\right)}{\partial \alpha_e}\Delta t & -R_b^e \Delta t & 0_{3x3} \\ 0_{3x3} & 0_{3x3} & I_{3x3} - \frac{\partial\left(R_\alpha b_g\right)}{\partial \alpha_e}\Delta t & 0_{3x3} & -R_\alpha \Delta t \\ 0_{3x3} & 0_{3x3} & 0_{3x3} & I_{3x3} & 0_{3x3} \\ 0_{3x3} & 0_{3x3} & 0_{3x3} & 0_{3x3} & I_{3x3} \end{bmatrix} \tag{7}$$

$$G_k^i = \begin{bmatrix} 0_{3x3} & 0_{3x3} & 0_{3x3} & 0_{3x3} & 0_{3x3} \\ R_b^e \Delta t & 0_{3x3} & 0_{3x3} & 0_{3x3} & 0_{3x3} \\ 0_{3x3} & R_\alpha \Delta t & 0_{3x3} & 0_{3x3} & 0_{3x3} \\ 0_{3x3} & 0_{3x3} & I_{3x3} & 0_{3x3} & 0_{3x3} \\ 0_{3x3} & 0_{3x3} & 0_{3x3} & I_{3x3} & 0_{3x3} \end{bmatrix} \tag{8}$$

Since the state transition and other matrices are now known, the predicted joint state and covariance of the overall swarm network is computed using standard EKF prediction equations as below. In these equations, the predicted and updated states are denoted by X_k^- and X_{k-1}^+, respectively. The corresponding predicted and updated covariance is denoted by P_k^- and P_{k-1}^+, respectively and Q_k denotes the process noise covariance.

$$X_k^- = X_{k-1}^+ + f\left(X_{k-1}^+, U_{k-1}, W_{k-1}\right)\Delta t \tag{9}$$

$$P_k^- = F_{k-1} P_{k-1}^+ F_{k-1}^T + G_{k-1} Q_{k-1} G_{k-1}^T \tag{10}$$

Although the above state and covariance prediction is performed in a centralized manner, the same could also be performed in a distributed manner because the joint state transition matrix is diagonal. The next section presents the framework for inclusion of measurements from GNSS, Wi-Fi, UWB and other neighbouring UAVs.

3.2 Measurement Models in a Cooperative Swarm

The measurements received by any UAV may include GNSS position (or pseudoranges), Wi-Fi measurements from static AP, UWB ranges from static nodes and relative ranges from other UAVs. Thus, the measurement vector for a UAV i can be expressed as follows.

$$z_k^i = \begin{bmatrix} \left(p_k^i\right)^T & d_k^{i,1} & d_k^{i,2} & . & . & d_k^{i,n} & c_k^{i,1} & c_k^{i,2} & . & . & c_k^{i,m} \end{bmatrix}^T \tag{11}$$

In the above equation, the position solution from a GNSS receiver on-board the i^{th} UAV is denoted by p_k^i. The range measurements received from either static UWB nodes or neighbouring UAVs is denoted by $d_k^{i,j}$, while the range derived from RSS value of the m^{th} AP is denoted by $c_k^{i,m}$. The joint measurement vector for the complete network is denoted as Z_k and is given by equation (12). The measurement models relating GNSS measurement and range derived from UWB or Wi-Fi, with the state of i^{th} UAV are given by equations (12) to (14). In these equations, the notations ε_k^d and ε_k^c denote the random errors in range measurements derived from UWB and Wi-Fi RSS measurements, respectively. The range

measurements derived from UWB are computed using TW-TOA (Two Way Time of Arrival) measurements, while the ranges derived from Wi-Fi RSS measurements make use of the path-loss models (Retscher and Tatschl 2016). Alternatively, fingerprinting based methods could also be employed for positioning using Wi-Fi measurements. However, such methods are very much dependent on the environment conditions and require a specialized training phase which is very much demanding in terms of the required investment.

$$Z_k = \begin{bmatrix} \left(z_k^1\right)^T & \left(z_k^2\right)^T & . & . & \left(z_k^N\right)^T \end{bmatrix}^T \tag{12}$$

$$d_k^{i,j} = \left\| r_k^i - r_k^j \right\| + \varepsilon_k^d \tag{13}$$

$$c_k^{w,i} = \left\| r_k^w - r_k^i \right\| + \varepsilon_k^c \tag{14}$$

The Wi-Fi methods based on path-loss models offer a simpler alternative as compared to fingerprinting methods. The path loss model for computing distance from RSS measurements is given in equation (17) and the complete process is discussed in section 4. The generalized measurement model incorporating all measurements received by all UAVs in the network is expressed by equation (15) where $h(X_k)$ denotes a measurement function and ε_k^z denotes a random error in the received measurements. The joint measurement matrix (given by the Jacobian of the measurement function) can be then computed according to the expression given in equation (16).

$$Z_k = h(X_k) + \varepsilon_k^z \tag{15}$$

$$H_k = \begin{bmatrix} H_{k,p}^1 & 0 & 0 & 0 & 0 \\ 0 & H_{k,p}^2 & 0 & 0 & 0 \\ . & . & . & . & . \\ . & . & . & . & . \\ 0 & 0 & 0 & 0 & H_{k,p}^N \\ \frac{\partial d_k^{1,2}}{\partial r_k^1} & . & . & . & \frac{\partial d_k^{1,2}}{\partial r_k^m} \\ . & . & . & . & . \\ \frac{\partial d_k^{i,j}}{\partial r_k^1} & . & . & . & \frac{\partial d_k^{i,j}}{\partial r_k^m} \\ . & . & . & . & . \\ \frac{\partial c_k^{w,i}}{\partial r_k^1} & . & . & . & \frac{\partial c_k^{w,i}}{\partial r_k^n} \end{bmatrix} \tag{16}$$

In the above equation, the matrix $H_{k,p}^i$ is a 3x3 identity matrix and relates the received GNSS position measurements and the position of the i^{th} UAV. The other terms can be computed using mathematical formulations given in equations (13) and (14) and are derived in Goel *et al.* (2017a). Using these matrices and the standard EKF update equations, the updated joint state of the whole swarm can be estimated. The next section explains the complete simulation methodology for indoor-outdoor cooperative localization.

4. SIMULATION SETUP FOR COOPERATIVE LOCALIZATION

The simulation setup includes five UAV platforms all of which are assumed to be equipped with sensors listed in Table 1. Of the five UAVs, one UAV (ID 1) is assumed to be flying in an indoor environment, i.e. in the complete absence of GNSS measurements. Further, it is assumed that the Wi-Fi AP and static UWB nodes are available in the environment, thus

providing additional measurements to all the UAVs. The precise location of Wi-Fi AP and UWB nodes is assumed to be known in advance. In addition, each UAV is able to measure relative range with respect to other UAVs using the on-board UWB sensor. The complete information is transmitted via an internet modem to a central server that computes the cooperative solution for all UAVs and transmits it back to the respective UAVs. The complete simulation scenario is depicted in Figure 2 to Figure 4. A plan view of the complete network is seen in Figure 2. A total of 5 UAVs are assumed with trajectories as shown in this Figure. The UAVs are assumed to be flying about 50 m apart so as to avoid any cases of UAV collisions. The locations of 14 UWB nodes (black circles) and 9 Wi-Fi AP (red circles) distributed randomly throughout the region are also seen in this Figure. Of the available static nodes, 4 Wi-Fi AP (AP3, AP4, AP6, AP7) and 2 UWB nodes are inside the building. The gyroscope measurements from one of the UAVs is shown in Figure 3. The velocity profile of the UAVs is shown in Figure 4. It is evident from these Figures that each UAV as well as the overall cooperative network is very dynamic with UAVs achieving a velocity of the order of 4 m/s. It is to be noted that the gyroscope and accelerometer measurements used in this simulation are from a real UAV flight. The assumed standard deviations in various measurements in this network are given in Table 2. This simulation assumes a fully connected network, i.e. each UAV is connected and able to communicate with all the other static nodes (UWB and Wi-Fi AP) as well as other UAVs.

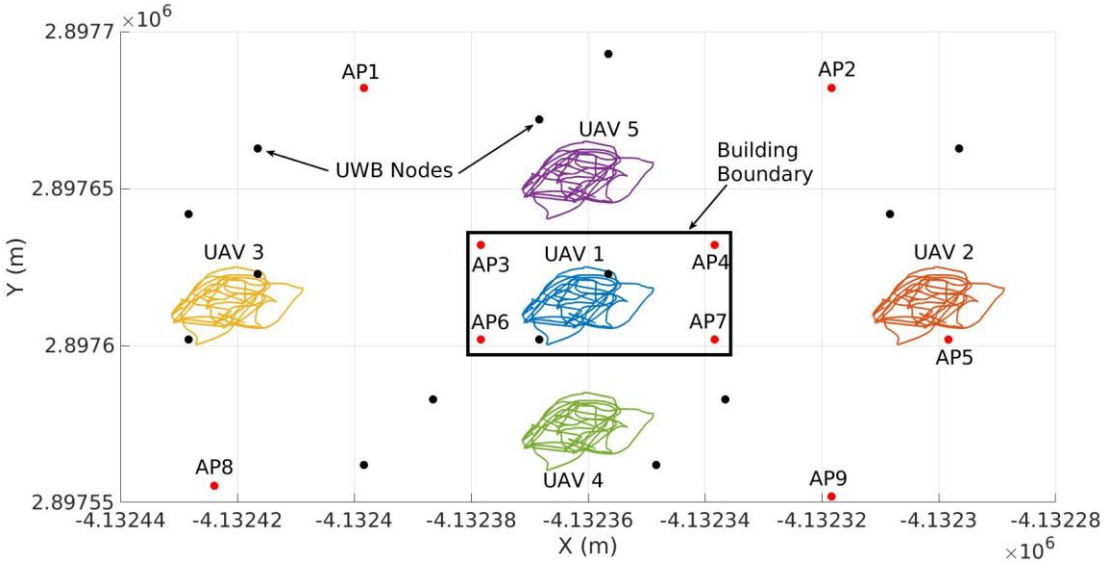

Figure 2: Plan view of the cooperative network with 5 UAVs, 14 static UWB nodes and 9 Wi-Fi AP.

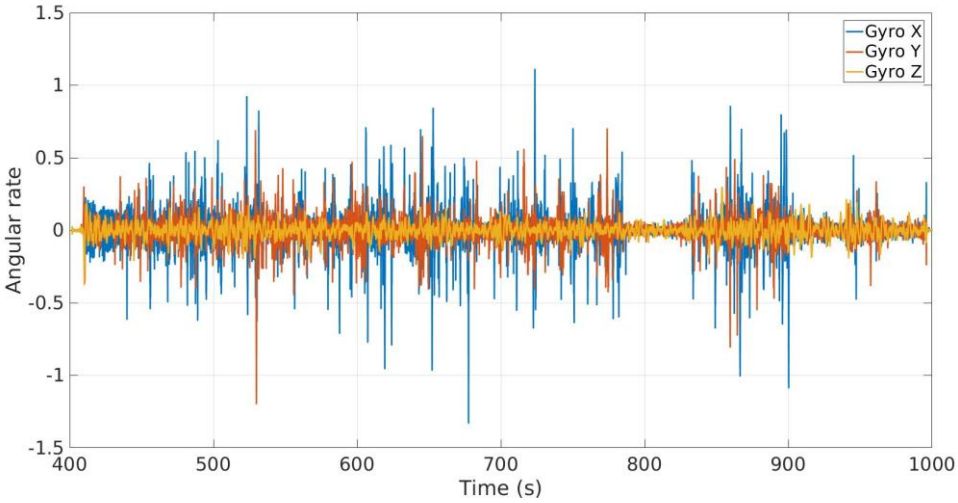

Figure 3: Gyroscope measurements for one of the UAVs.

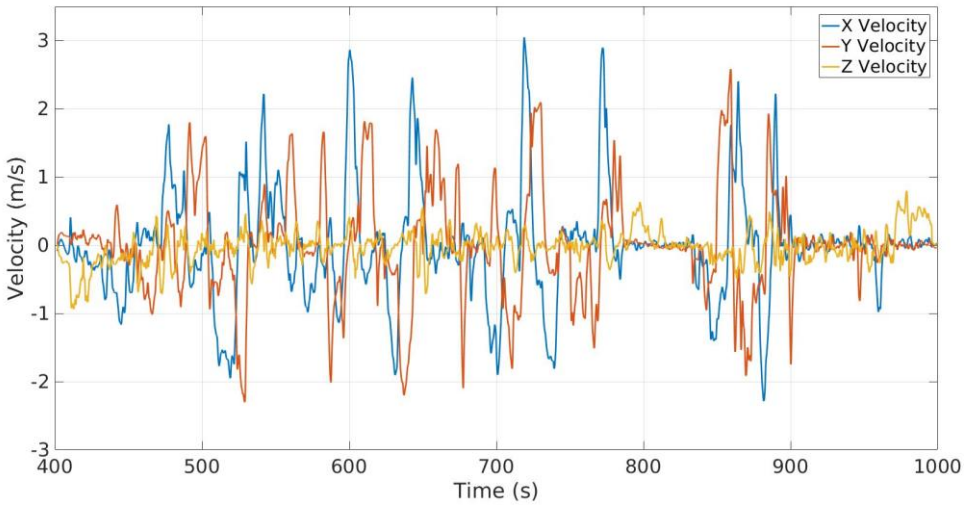

Figure 4: Velocity plot for one of the UAVs.

Table 2: Assumed standard deviation in the measurements used in the simulation.

Measurement type	Assumed standard deviation
GNSS position (3D)	2.5 m
UWB range measurement (LOS)	0.5 m
UWB range measurement (NLOS)	2 m
RSS measurement	2 dBm

The trajectory data presented here is from an actual flight data. For simulation purposes, it is considered as the reference ground truth. A Gaussian random error with standard deviation of 2.5 m is added in the ground truth data to obtain the simulated GNSS measurements for the UAVs. The UWB range measurements are simulated using the trajectory information of the UAVs and known locations of UWB nodes. For the LOS (line of sight) conditions, a standard deviation of 0.5 m is assumed in the range measurement. It has been observed that in NLOS conditions, the error in the range measurements increases. Therefore, the range accuracy is assumed to be 2 m for NLOS conditions. In this particular simulation NLOS conditions arise in the cases of interaction of UAV 1 with other UAVs, interactions between UAV 1 and other static UWB nodes that are installed outside the building and interactions between UWBs inside the building with UAVs outside the building. The Wi-Fi data is simulated on the basis of a path loss model given in equation (17). This empirical model for signal propagation translates the received RSS to distance between the transmitter and receiver and provides a suitable approximation in indoor environments (Retscher and Tatschl 2016).

$$P(d) = P_o - 10\gamma \log_{10}(d) \tag{17}$$

In this equation, P and P_o denote the received empirical and reference RSS at 1 m, respectively. The damping factor and distance is denoted by γ and d, respectively. It is assumed that the frequency of Wi-Fi signals is 2.45 GHz and thus, a value of $\gamma = 4.2$ as determined by authors in Retscher and Tatschl (2016) for indoor environments is used in this simulation. Once the RSS values are obtained using the above model, a random Gaussian error with standard deviation of 2 dBm is added to compute the recorded measurements. These RSS measurements are received by the Raspberry Pi on-board the UAVs. An example of the simulated RSS measurements from three APs generated using the above method is shown in Figure 5. It can be seen that this simulated data appears similar to the real RSS vs. distance plot demonstrated by the authors in Retscher and Tatschl (2016). This provides an overall validation regarding the adopted Wi-Fi simulation methodology and demonstrates that the simulated RSS measurements are very much realistic. The RSS measurements thus

generated are used to derive distances between Wi-Fi AP and UAVs using the above mentioned path loss model. Alternatively, the above model can be directly incorporated in the measurement process. The positioning solution for all UAVs is obtained using the developed framework and is presented and analysed in the next section.

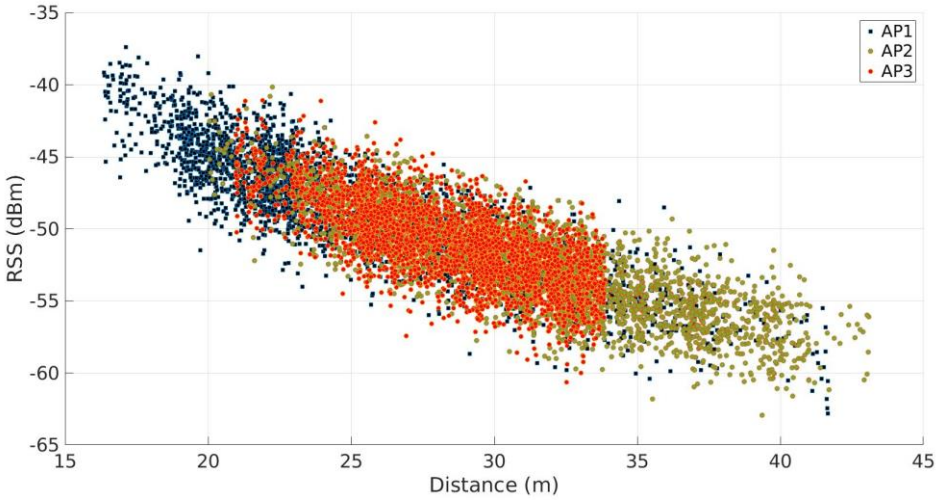

Figure 5: Simulated RSS measurements received by a UAV from three different APs.

5. RESULTS AND DISCUSSION

The positioning solution of all UAVs (including the UAV without GNSS) is estimated jointly using the framework presented in section 3. The positioning solution of UAV 1 that is operating indoors (i.e. in the absence of GNSS measurements) is processed using both UWB and Wi-Fi measurements together as well as UWB and Wi-Fi measurements separately. This is done to analyse the advantage of including UWB measurements in a cooperative system that relies primarily on the Wi-Fi measurements only. The total error in the estimated trajectory of UAV 1 in the presence of UWB and Wi-Fi, UWB only and Wi-Fi only measurements is shown in Figure 6 and two zoomed views (view 1 and view 2) of the same Figure are shown for better clarity in Figure 7 and Figure 8, respectively.

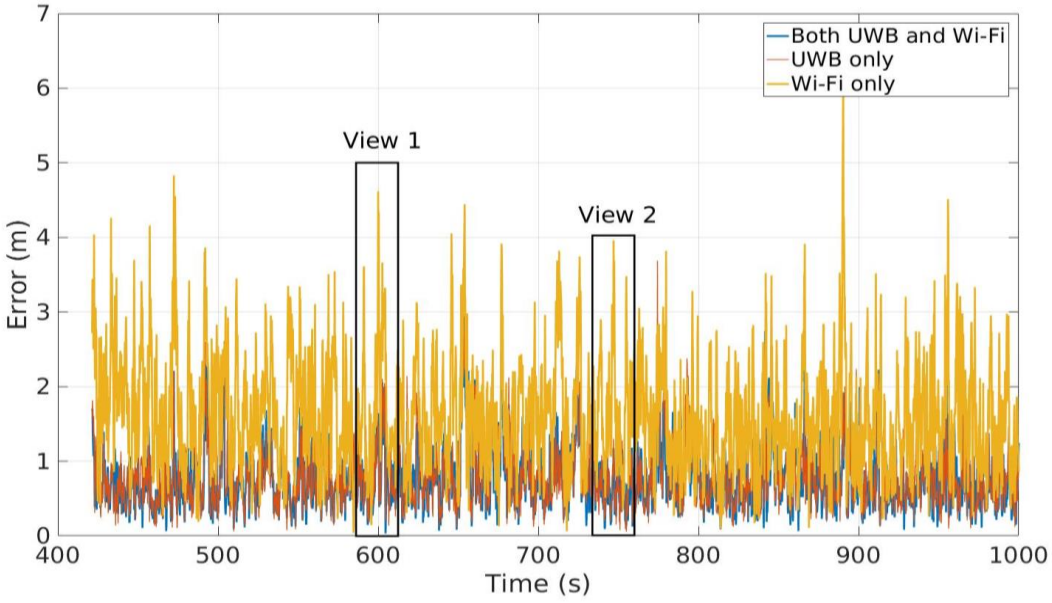

Figure 6: Error plot for positioning solution of UAV 1. This UAV is operating indoors.

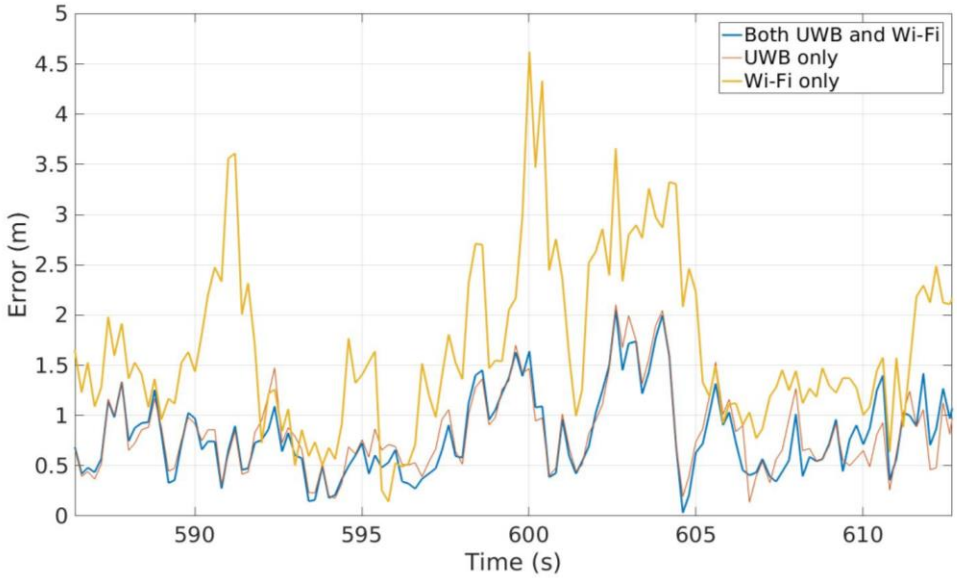

Figure 7: View 1: Zoomed view of Figure 6.

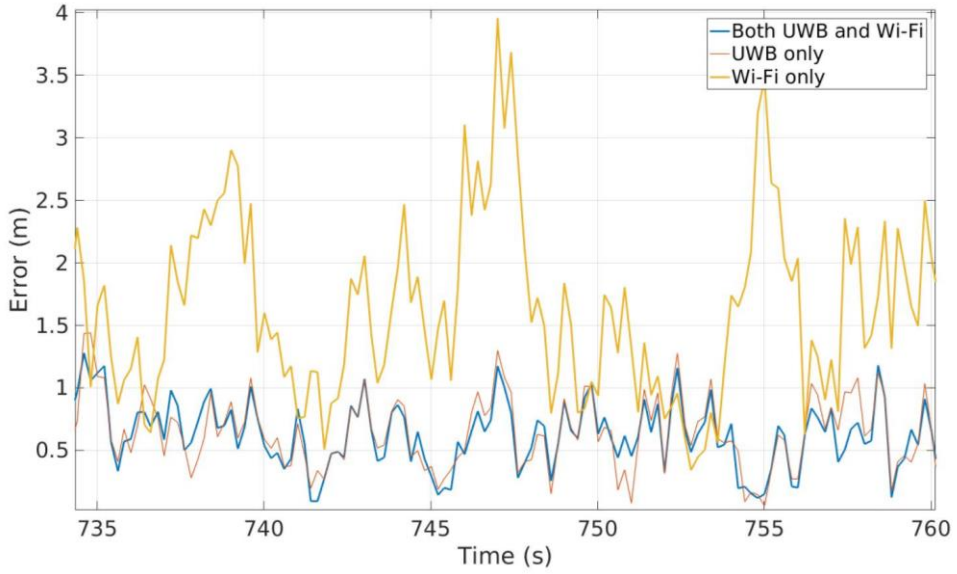

Figure 8: View 2: Zoomed view of Figure 6.

An important observation that can be made from these Figures is that the trajectory solution does not diverge in the absence of GNSS measurements. This demonstrates that the proposed cooperative localization solution has been effective in restraining the trajectory in indoor environments. Further, it can be noted that the joint UWB and Wi-Fi measurement solution is much better as compared to the 'Wi-Fi only' solution and is only marginally better than the 'UWB only' solution. This can be attributed to the fact that the UWB range measurements are more precise than the range measurements derived from Wi-Fi RSS measurements. It is observed that a standard deviation of 2 dBm in the RSS measurements results in a standard deviation of about 2.2 m at a distance of 20 m and 10 m at a distance of about 100 m. This is significantly larger as compared to a standard deviation of 0.5 m in LOS and 2 m in NLOS environments in UWB measurements. Since, a majority of the Wi-Fi APs are at a larger distance from the UAVs, the range observations derived from Wi-Fi RSS measurements are not as precise as the UWB measurements. This demonstrates that a significant improvement in the localization solution can be expected after inclusion of UWB measurements in the cooperative network. Conversely, inclusion of Wi-Fi measurements in a UWB based cooperative network may result in marginal improvement in the overall accuracy. This

improvement is primarily dependent on the distance of the Wi-Fi APs from the UAVs. The APs that are closer to the UAVs result in a larger improvement in the trajectory solution as compared to the APs that are further away. A colour coded trajectory map of UAV 1 for the case when both UWB and Wi-Fi measurements are used together is shown in Figure 9.

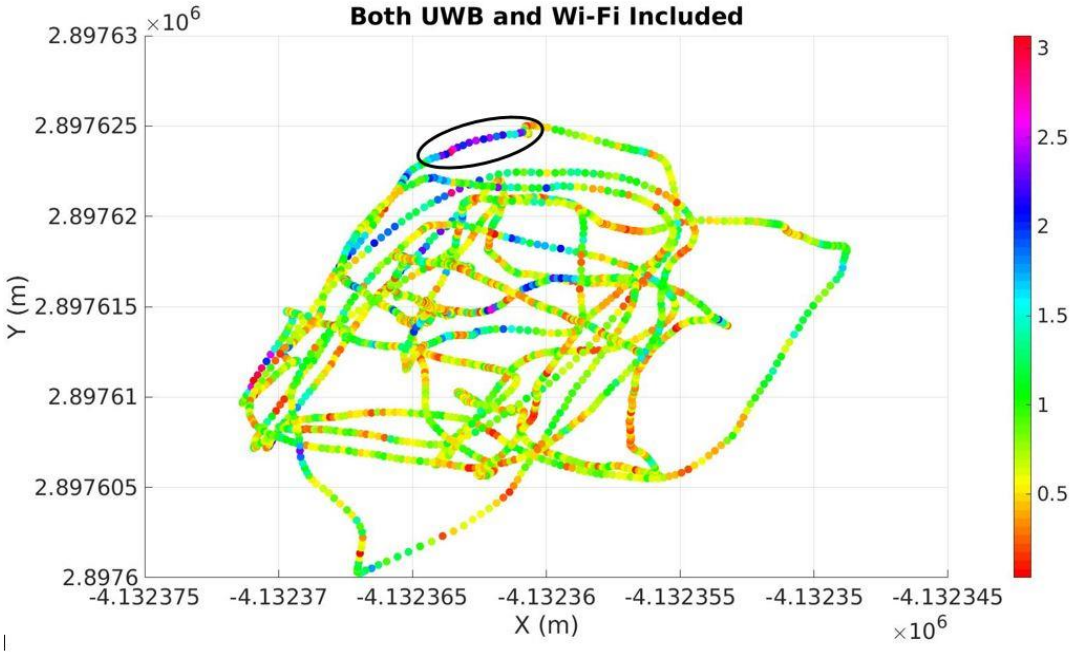

Figure 9: Colour coded (plan) trajectory map of UAV 1. The trajectory is colour coded according to the error in the positioning solution.

This trajectory map is colour coded according to the error in the positioning solution and the corresponding colour scale is also shown in the same Figure. It can be seen that the positioning error remains well below 2 m, in a major part of the trajectory. During one section (marked with an ellipse), the error varies from about 2 to 3 m. This is most likely due to the reason that the UAV performed certain unexpected manoeuvres during this period that could not be modelled correctly. This paper uses a constant process noise that is optimized for the overall dynamics of the UAV. This unexpected manoeuvre of the UAV can be incorporated well if an adaptive process noise is introduced in the proposed system. The overall performance of the developed system can evaluated using the frequency (scaled probability density) and the cumulative probability plot of the error in the estimated trajectory and are shown in Figure 10 and Figure 11, respectively. It can be observed from these Figures that the overall performance of the 'Wi-Fi only' solution is considerably poorer as compared to the 'UWB only' or 'Both UWB and Wi-Fi' solution. The overall mean RMSE (Root Mean Square Error) in the 'UWB and Wi-Fi', 'UWB only' and 'Wi-Fi only' solutions is about 0.88 m, 0.92 m and 1.77 m, respectively, while the mode of the error in the three solutions is about 0.58 m, 0.57 m and 1.32 m, respectively. Further, it can be observed that the UAV is able to achieve positioning accuracy of 5 m more than 99% of the time during the flying mission in the absence of GNSS measurements for all the above mentioned three cases. The 'Wi-Fi only' solution achieves an accuracy of 2 m about 70% of the time, while both 'UWB only' and 'UWB and Wi-Fi' solutions achieve the same accuracy more than 95% of the time. This can be attributed to the quality of the range measurements derived from Wi-Fi RSS observations being poorer as compared to the range measurements from UWB. Until this point, it is assumed that only one of the UAVs in the network did not have GNSS measurements. The effect of GNSS availability in a cooperative network on the localization performance of the UAV that is operating indoors is presented in Figure 12. This is presented

for the case when only Wi-Fi measurements from static APs and relative range measurements from the dynamic UAVs are shared in the network. In Figure 12, a GNSS availability of 40% means that only two of the five UAVs can receive GNSS measurements.

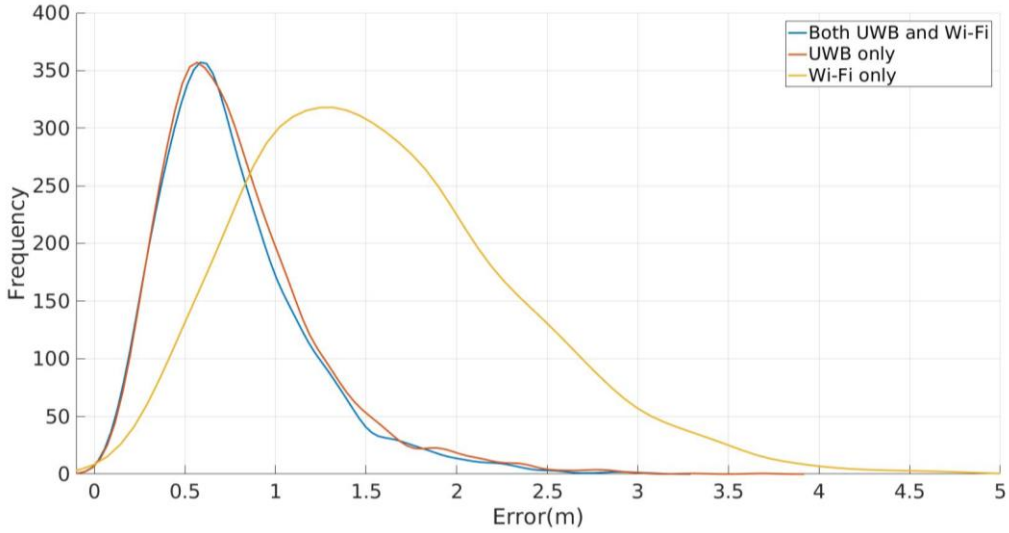

Figure 10: Frequency plot of the error in positioning solution of UAV 1.

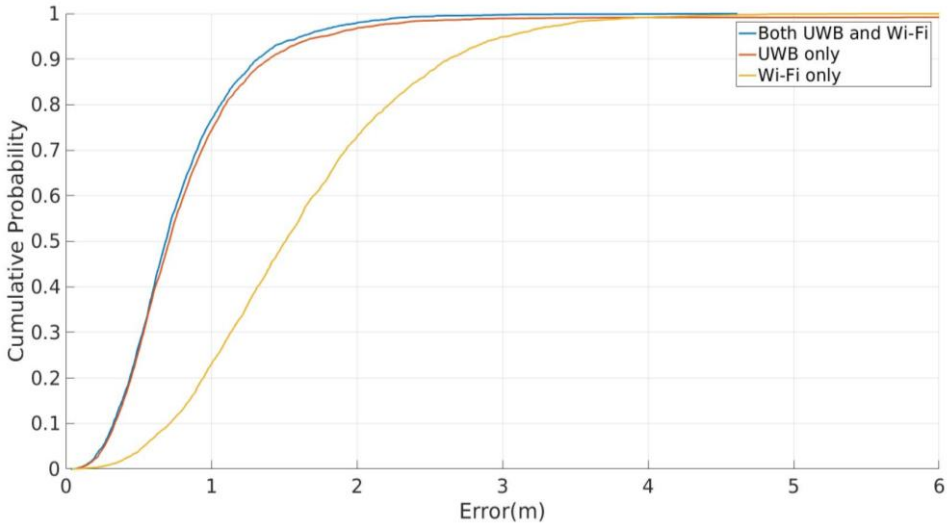

Figure 11: CDF plot of error in the positioning solution for the UAV (ID 1) that is operating indoors.

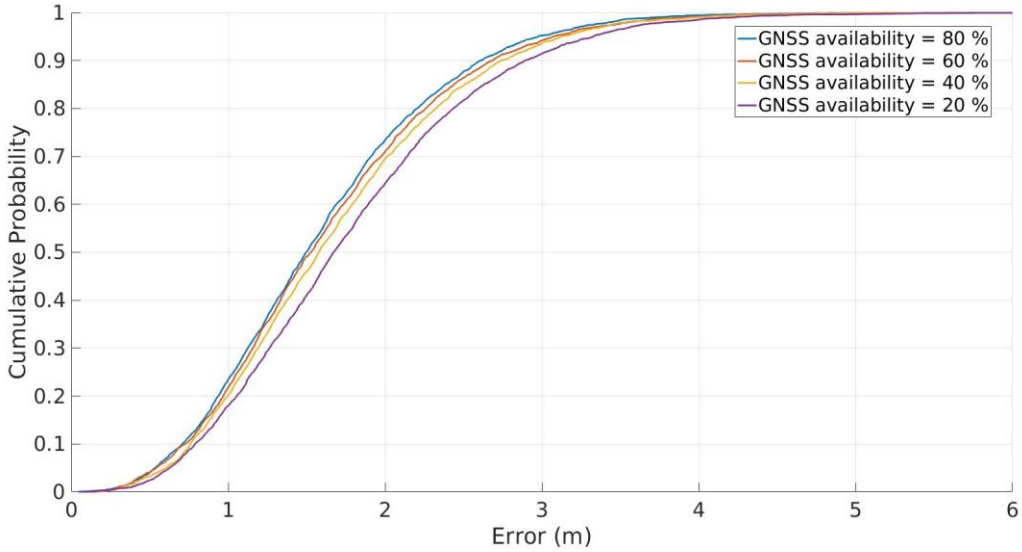

Figure 12: Effect on the localization performance of UAV 1 with change in GNSS availability in the network. The static UWB nodes are not considered in this simulation.

It can be observed that the localization performance of UAV 1 is affected by the availability of GNSS measurements to its neighbouring UAVs. Highest accuracy (3 m about 95% of the time and 2 m about 75% of the time) is achieved when GNSS availability is 80%, i.e. all remaining 4 UAVs can receive GNSS measurements. This degrades to about 90% and 65% at 3 m and 2 m, respectively for the case when GNSS availability is reduced to 20%, i.e. only one UAV (of the five UAVs) in the network can receive GNSS measurements. This highlights that the availability of GNSS measurements to neighbouring UAVs affect the localization performance of all other UAVs. In this specific case the degradation is not too large because of the continuous availability of Wi-Fi RSS measurements from the APs. The next section presents the conclusions of this paper and scope of future work.

6. CONCLUSIONS AND FUTURE WORK

This paper has developed and demonstrated a framework for an indoor-outdoor cooperative localization system that integrates measurements from static UWB nodes, Wi-Fi APs as well as dynamic UAV platforms. The proposed system integrates low cost GNSS, IMU, UWB and Raspberry Pi. In addition, a low-cost camera is also integrated in the system but is not used for processing in this paper. The framework utilized a centralized EKF for cooperative positioning and evaluated the performance of a UAV in cooperative network that is operating in the absence of GNSS measurements (indoor environment). The simulated data used in this paper includes a real flight data of a UAV (including GNSS and IMU measurements) and simulated Wi-Fi RSS and UWB measurements. The simulations demonstrated that the proposed system can achieve accuracies of the order of 2 to 5 m in indoor environments by using either Wi-Fi, or UWB or both measurements, in addition to the relative measurements from neighbouring UAVs. Using only Wi-Fi measurements (along with measurements from other UAVs), the proposed system could achieve accuracy ~ 3 m about 95% of the time while, this accuracy improves to about 1.5 m for the case of 'UWB only' and 'UWB and Wi-Fi' measurements. The inclusion of Wi-Fi measurements in a UWB only cooperative system results in a marginal improvement in the localization accuracy. Conversely, inclusion of measurements from static UWB nodes in a Wi-Fi only cooperative network significantly improves the localization accuracy of the overall network. Further, it is observed that overall positioning accuracy of the network degrades with decrease in the GNSS availability. It is observed that performance of a UAV that is operating without GNSS is very much dependent on the availability of GNSS measurements to its neighbouring UAVs. In summary, it is found that the proposed system can achieve navigation level accuracies (~ 2 m to 5 m) in GNSS challenging environments. The developed system has applications in exploration, search and rescue missions, assisted navigation, disaster management, situational awareness, etc. The future work is focused at experimental realization and validation of the simulation results presented in this paper and extension of the proposed centralised system to a distributed cooperative swarm. Since, a low-cost camera is also integrated in the developed system, the camera measurements could also be incorporated in the developed system. Hence, the future work would also attempt to perform a cost-benefit analysis of addition of camera measurements in the developed cooperative network.

REFERENCES

Bailey T, Bryson M, Mu H, Vial J, McCalman L, Durrant Whyte H (2011) Decentralised cooperative localization for heterogeneous team of mobile robots, *Proc. IEEE International Conference on Robotics and Automation*, Shanghai, China, pp. 2859-2865, DOI: 10.1109/ICRA.2011.5979850.

Caceres M. A, Penna F, Wymeersch H, Garello R (2010) Hybrid GNSS-terrestial cooperative positioning via distributed belief propagation, *GLOBECOM-IEEE Global Telecommunications Conference,* pp 1-5, DOI: 10.1109/GLOCOM.2010.5683684.

Carrillo-Arce L. C., Nerurkar E. D., Gordillo J. L., Roumeliotis S. I. (2013) Decentralized multi-robot cooperative localization using covariance intersection, *2013 IEEE/RSJ International Conference on Intelligent Robots and Systems*, pp. 1412-1417.

Goel S (2017) A Distributed Cooperative UAV Swarm Localization System: Development and Analysis, *Proceedings of the 30th International Technical Meeting of The Satellite Division of the Institute of Navigation (ION GNSS+ 2017),* Portland, Oregon, September 25-29, 2017, pp. 2501-2518.

Goel S, Kealy A, Gikas V, Retscher G, Toth C, Brzezinska DG, Lohani B (2017a) Cooperative Localization of Unmanned Aerial Vehicles Using GNSS, MEMS Inertial and UWB Sensors, *Journal of Surveying Engineering* 143(4), DOI:10.1061/(ASCE)SU.1943-5428.0000230.

Goel S, Kealy A, Lohani B (2016a), Cooperative UAS Localization using low cost sensors, *ISPRS Annals of Photogrammetry Remote Sensing and Spatial Information Science,* ISPRS Congress, Prague, Czech Republic, III-1:183-190.

Goel S, Kealy A, Lohani B (2016b), Infrastructure vs. Peer to Peer Cooperative Positioning: A comparative analysis, *Proceedings of the 29th International Technical Meeting of The Satellite Division of the Institute of Navigation (ION GNSS+ 2016),* Portland, Oregon, pp. 1125-1137.

Goel S, Kealy A, Lohani B, Retscher G (2017b) A Cooperative Localization System for Unmanned Aerial Vehicles: Prototype Development and Analysis, *Proceedings of 10th International Symposium on Mobile Mapping Technology (MMT 2017),* Cairo, Egypt, May 6-8, 2017.

Goel S, Kealy A, Retscher G, Lohani B (2016c) Cooperative P2I Localization using UWB and Wi-Fi, *Proceedings of International Global Navigation Satellite Systems (IGNSS) Association Conference 2016,* Sydney Australia, December 6-8, 2016.

Indelman V, Gurfil P, Rivlin E, Rotstein H (2011) Distributed vision-aided cooperative localization and navigation based on three-view geometry, *2011 IEEE Aerospace Conference*, DOI: 10.1109/AERO.2011.5747546.

Karam N, Chausse F, Romuald A, Chapuis R (2006) Localization of a Group of Communicating Vehicles by State Exchange, *Proc. 2006 IEEE/RSJ Int. Conf. Intell. Robot. Syst.*, pp. 519–524, October 9 - 15, 2006, Beijing, China.

Madhavan R, Fregene K, Parker, L. E (2002) Distributed heterogeneous outdoor multi-robot localization, P*roc. 2002 IEEE Int. Conf. Robot. Autom. (Cat. No.02CH37292)*, vol. 1, pp. 374–381, 2002.

Retscher G, Tatschl T (2016) Indoor positioning using Wi-Fi lateration - Comparison of two common range conversion models with two novel differential approaches, *Proc. Fourth International Conference on Ubiquitous Positioning, Indoor Navigation and Location Based Services (UPINLBS),* Shanghai, China, November 3-4, 2016, DOI: 10.1109/UPINLBS.2016.7809967.

Roumeliotis S. I., Bekey G. A. (2002) Distributed multirobot localization, *IEEE Trans. Robot. Autom.*, vol. 18, no. 5, pp. 781–795.

Savic V, Población A, Zazo S, García M (2010) Indoor Positioning Using Nonparametric Belief Propagation Based on Spanning Trees, *EURASIP J. Wirel. Commun. Netw.*, vol. 2010, no. 1, DOI: 10.1155/2010/963576.

Schauer L, Dorfmeister F, Maier M (2013) Potential and limitations of Wi-Fi positioning using time-of-flight, *Proc. International Conference on Indoor Positioning and Indoor Navigation (IPIN 2013),* October 28-31, 2014, pp. 28-31, DOI: 10.1109/IPIN.2013.6817861.

Xiao W, Ni W, Toh Y. K. (2011) Integrated Wi-Fi fingerprinting and inertial sensing for indoor positioning, *Proc. International Conference on Indoor Positioning and Indoor Navigation (IPIN 2011),* September 21-23, 2011, DOI: 10.1109/IPIN.2011.6071921.